

**Vector and tensor polarization lifetimes for a stored deuteron beam**B. v. Przewoski, V. A. Anferov, H. O. Meyer, P. Schwandt, and E. J. Stephenson  
*Indiana University Cyclotron Facility, Bloomington, Indiana 47405, USA*V. S. Morozov, Z. B. Etienne,\* M. C. Kandes, M. A. Leonova, D. W. Sivers,† and K. Yonehara  
*Spin Physics Center, University of Michigan, Ann Arbor, Michigan 48109-1120, USA*

(Received 8 May 2003; published 2 October 2003)

The time dependence of the vector and tensor polarization of a 270 MeV stored deuteron beam was measured near a depolarizing resonance, which was induced by an oscillating, longitudinal magnetic field. The distance to the resonance was varied by changing the oscillation frequency. The measured ratio of the polarization lifetimes is  $\tau_{\text{vector}}/\tau_{\text{tensor}} = 1.9 \pm 0.2$ . Assuming that the effect of the resonance is to induce transitions between magnetic substates  $m_J$ , we find that the transition rate between neighboring states (+1 and 0 or -1 and 0) is four times higher than between the states with  $m_J = +1$  and  $-1$ .

DOI: 10.1103/PhysRevE.68.046501

PACS number(s): 29.27.Bd, 29.27.Hj, 41.75.Ak, 29.20.Dh

**I. INTRODUCTION**

Since polarized beams were first cooled in a storage ring, the question of how long the stored beam remains polarized has been of considerable interest [1]. It was found that usually the polarization lifetime is large compared to the beam lifetime; however, as a depolarizing resonance is approached, the polarization lifetime decreases sharply. Previously, the polarization lifetime has been studied for stored proton beams as a function of the distance from intrinsic as well as induced depolarizing resonances [2,3].

With the recent interest in deuteron beams for nuclear physics experiments (e.g., at COSY [4]), the behavior of the polarization of stored spin-1 particles has become important. In particular, the question arises whether, in the vicinity of a depolarizing resonance, the lifetimes of vector and tensor polarization differ.

In a recent experiment at the Indiana Cooler, we measured the vector and tensor polarization of a 270 MeV stored deuteron beam before and after adiabatically crossing an induced depolarizing resonance [5]. For a slow crossing rate, it was found that the sign of the vector polarization is reversed (flipped) while the sign of the tensor polarization is unchanged. At a slower crossing rate, corresponding to an incomplete rotation of the spin closed orbit, the observed vector polarization was zero and the tensor polarization reversed sign but was reduced by a factor of 2 ([5], Fig. 3, and [6]).

Since vector and tensor polarization behave so differently when crossing a depolarizing resonance, it can be expected that the polarization lifetimes also differ. The present article describes the measurement of the vector and tensor polarization lifetime near an induced depolarizing resonance at 270 MeV.

**II. PREPARATION OF THE BEAM**

Polarized deuterons from a pulsed atomic beam source (CIPIOS) were accelerated to 100 MeV in the Indiana Cooler

injector synchrotron (CIS) and then transferred to the Cooler where they were further accelerated to 270 MeV. The betatron tunes of the Cooler were adjusted to avoid the  $G\gamma + 5 = \nu_y$  intrinsic resonance during acceleration. The fractional betatron tunes measured after acceleration were  $Q_x = 0.188$  and  $Q_y = 0.214$ .

In order to minimize systematic errors, the experiment was carried out with beams of different combinations of vector and tensor polarization (called “beam states” in the following), as well as with an unpolarized beam. The four beam states were injected into the Cooler in sequence, using a different state for each new cycle. Resetting the Cooler magnets prior to injection ensured that no beam from the previous cycle remained in the ring. In the following we describe briefly how the polarized beam was prepared. More information about the polarized source (CIPIOS) can be found in [7].

The process starts with the dissociation of deuterium atoms. These atoms emerge through a cooled nozzle and then encounter two stages consisting of a set of permanent sextupole magnets followed by a rf transition unit. These devices affect the populations of the six hyperfine states of the deuterium atom. In the following, we use the conventional numbering of these states in order of decreasing energy in a non-zero magnetic field [8]. The sextupole magnets separate the atoms according to their electron polarization, i.e., states 1,2,3 are focused and states 4,5,6 are defocused. The rf transitions cause the inversion of the populations of pairs of states. The first stage is equipped with a medium field transition (MFT) and the second stage with a weak field transition (WFT), immediately followed by a strong field transition (SFT). Table I illustrates how the four different beam states (column 1) are prepared. Columns 2 through 6, respectively, list the hyperfine states that remain after the first sextupole, the states that are exchanged in the MFT, the states that remain after the second sextupole, and the transitions made in the WFT and the SFT. Finally, the hyperfine states that are populated when the beam emerges from the source are listed in column 7. The atoms are ionized in a strong field (where the spins of the electrons and the nuclei are decoupled). This leads to the nominal vector ( $P_z$ ) and tensor ( $P_{zz}$ ) polarization shown in columns 8 and 9. For a number of

\*Also at Indiana University, Bloomington, IN 47408.

†Also at Portland Physics Institute, Portland, OR 97201.

TABLE I. Sequence of sextupole separations and hyperfine transitions made in CIPIOS. For details see text.

Beam state	Sequence of transitions						$P_z$	$P_{zz}$
	Sextupole 1	MFT	Sextupole 2	WFT	SFT	Final states		
1	1,2,3	3 4	1,2		2 6	1,6	1	1
2	1,2,3	1 4	2,3	2 4		3,4	-1	1
3	1,2,3	1 4	2,3		2 6	3,6	0	1
4	1,2,3	1 4	2,3		3 5	2,5	0	-2

reasons, the actual polarizations are less than their nominal values: after acceleration in the Cooler the measured vector polarization (beam states 1 and 2) typically was  $\pm 0.6$ , the tensor polarization in beam states 1–3 was  $+0.8$ , and the tensor polarization in beam state 4 was  $-1.6$ .

### III. SPIN MOTION

In a ring with only vertical fields the magnetic moments of the beam particles precess about the vertical direction. The eigenvector of the precession of the magnetic moment in a single revolution around the ring is called the spin closed orbit. The precession frequency of the magnetic moment in the particle rest frame, the spin tune, is given by  $\nu_s = G\gamma$  where  $G = g - 1$  is the anomalous magnetic moment ( $G_{\text{deuteron}} = -0.1430$ ) and  $\gamma$  is the usual relativistic Lorentz factor. A depolarizing resonance occurs when nonvertical magnetic fields are encountered in resonance with the spin tune. A depolarizing resonance can be induced by a longitudinal oscillating magnetic field. On resonance, the frequency of the oscillating field is given by  $f_r = f_c(k \pm \nu_s)$  where  $f_c$  is the circulation frequency of the stored beam and  $k$  is an integer. Far away from the resonance the spin closed orbit is vertical. As the resonance is approached the spin closed orbit tilts and precesses around the vertical direction. On resonance, the tilt is  $\pi/2$  and the spin closed orbit lies in the ring plane. Depolarization occurs because near a resonance the spin motion becomes sensitive to the betatron amplitude of individual particles and is no longer coherent.

### IV. EXPERIMENT

#### A. Setup

The experiment was performed at the Indiana Cooler. A layout of the setup is shown in Fig. 1. The target consists of an open ended tube, 1.2 cm in diameter and 27 cm long, made from 0.05 mm thick aluminum. Hydrogen gas is fed into the center of this target cell, resulting in a target thickness of  $\sim 5 \times 10^{13}$  atoms/cm<sup>2</sup>. The outgoing proton and deuteron from *pd* elastic scattering were detected in coincidence in a stack consisting of a 0.635 cm thick  $\Delta E$  scintillator (*F*), two wire chambers (WC1, WC2), and a 15.24 cm thick stopping scintillator (*K*) [9].

#### B. Event selection

Elastically scattered events were distinguished from breakup events and from background originating from the

cell wall by the following software conditions. Two opposite elements of the stopping detector were required to have a signal. A least- $\chi^2$  fit to the wire chamber hit pattern had to be consistent with two prongs having a common vertex. This vertex was restricted to the target position. The correlation between the polar angles of the two prongs had to be consistent with *pd* elastic scattering and the azimuthal angle difference was required to be within  $\pm 10^\circ$  of  $180^\circ$ . In addition, the energy deposited in the stopping scintillator for both prongs and the angles measured by the wire chambers had to be consistent with *pd* scattering. For the analysis that follows, events in the center-of-mass angle range  $90^\circ \leq \theta_{\text{c.m.}} \leq 130^\circ$  were used.

#### C. Polarization measurement

A description of the formalism to describe spin-1 polarization and of the method to measure vector and tensor analyzing powers with polarized deuterons can be found in the literature [10,11]. The spin-dependent cross section is given by

$$\sigma = \sigma_0 [1 + 2iT_{11} \text{Re}(it_{11}) + T_{20}t_{20} + 2T_{21} \text{Re}(t_{21}) + 2T_{22} \text{Re}(t_{22})]. \quad (4.1)$$

Here,  $\sigma_0$  is the unpolarized cross section,  $iT_{11}$  and  $T_{2k}$  are

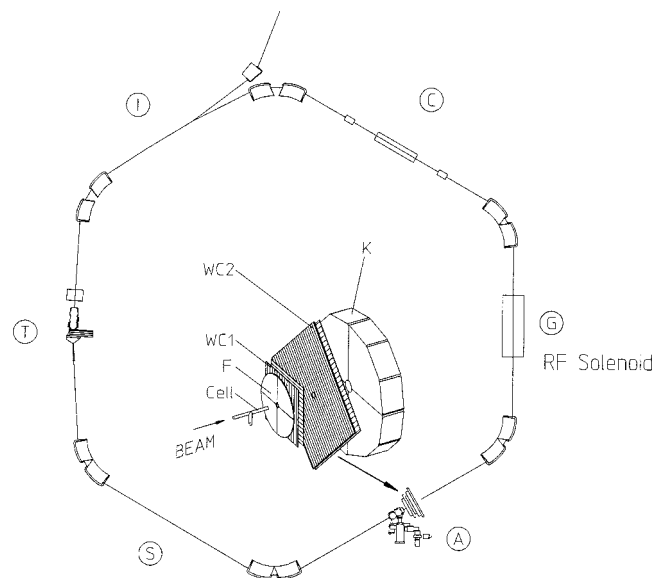


FIG. 1. Indiana University Cyclotron Facility Cooler ring and experimental setup. The components are described in the text.

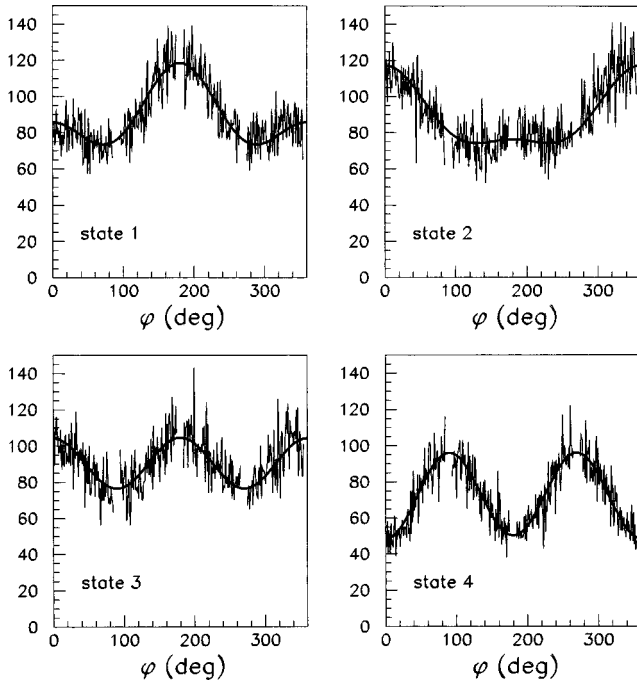


FIG. 2. Azimuthal count rate distributions for beam states 1–4. The lines are fits using Eq. (4.1) and the known vector and tensor analyzing powers.

the vector and tensor analyzing powers, and  $it_{11}$  and  $t_{2k}$  the corresponding beam moments, which are related in a known way to the polarizations  $P_z$  and  $P_{zz}$  of the beam. The beam moments depend on the orientation of the symmetry axis of the polarized ensemble (called the spin alignment axis) with respect to the scattering plane. In our case, with a vertical spin alignment axis, the  $t_{21}$  moment vanishes,  $it_{11}$  is proportional to  $\cos\phi$ , where  $\phi$  is the azimuth of the scattering plane,  $t_{22}$  is proportional to  $\cos(2\phi)$ , and  $t_{20}$  does not depend on  $\phi$ . In the present experiment we make use of the  $\phi$  dependence of the observed yields to pick out the terms  $it_{11}iT_{11}$  and  $t_{22}T_{22}$  in Eq. (4.1), which for beam states 1 and 2 are present simultaneously. Typical  $\phi$  distributions for the four beam states are shown in Fig. 2. Note that the offset of the  $\phi$  distribution is smaller for state 4, because the magnitude of  $t_{20}$  is about twice as large as for the other beam states. Each term in Eq. (4.1) is the product of a beam moment and an analyzing power. The analyzing powers of  $pd$  scattering at 270 MeV are known [12]. Averaging over the  $\theta$  acceptance yields the effective analyzing powers  $iT_{11} = -0.31$ ,  $T_{20} = -0.22$ , and  $T_{22} = -0.28$ . Thus, the moments  $it_{11}$  and  $t_{22}$  are deduced and the vector and tensor polarizations  $P_z$  and  $P_{zz}$  are obtained.

#### D. Induced resonance

The rf solenoid used to generate an oscillating magnetic field along the beam axis has been described elsewhere [13]. In this experiment, the rms value of the field integral was  $\int B dl = 0.7 \text{ T mm}$  when the solenoid was operated at full power. On resonance (see Sec. III) the solenoid frequency is given by  $f_{\text{sol}} = f_c(1 + \nu_s)$ . The circulation frequency of the

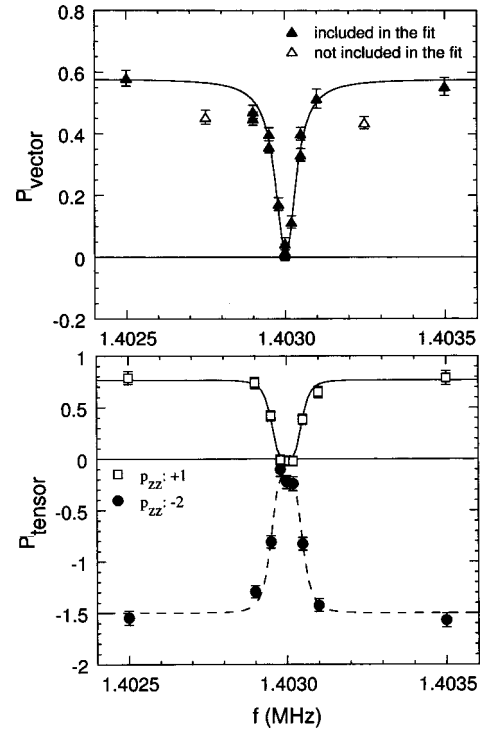


FIG. 3. Vector and tensor polarizations as a function of solenoid frequency. The lines are least- $\chi^2$  fits of first- and second-order Lorentzians to the vector and tensor polarizations, respectively.

deuterons in the Cooler was  $f_c = 1\,677\,551 \text{ Hz}$ . From  $f_c$  and the known circumference of the Cooler of  $86.77 \pm 0.01 \text{ m}$  [14], one obtains  $\gamma = 1.14388$  and  $\nu_s = G\gamma = -0.16356$ . The expected resonance frequency of the solenoid is then  $f_{\text{sol}} = 1\,403\,171 \pm 10 \text{ Hz}$ . Experience shows that the calculated frequency is close to the actual resonance frequency, but an experimental determination is still necessary. In the first step, the resonance is located approximately by a method described in [15]. The precise determination of the resonance location requires a measurement of the beam polarization as a function of solenoid frequency. This was done as follows. After accelerating and cooling the stored beam, the rf solenoid was turned on by linearly ramping the amplitude from zero to full power within 50 ms. The solenoid was then operated for 1 s, after which the amplitude was ramped down, mirroring the turn-on procedure. This was followed by the polarization measurement. Figure 3 shows the vector polarization from beam states 1 and 2, the positive tensor polarization, averaged over beam states 1–3, and the negative tensor polarization from beam state 4 as a function of solenoid frequency. The curves in Fig. 3 are first- and second-order Lorentzian fits with widths of  $75 \pm 4$  and  $101 \pm 4 \text{ Hz}$  for the vector and tensor polarizations, respectively. The central resonance frequency is  $f_{\text{sol}} = 1\,403\,002 \pm 14 \text{ Hz}$ .

#### V. MEASUREMENT

The polarization lifetime is measured using the following procedure. After the beam is injected, accelerated, and cooled, the solenoid is turned on and left on while data are taken. This is done with all four beam states and with the

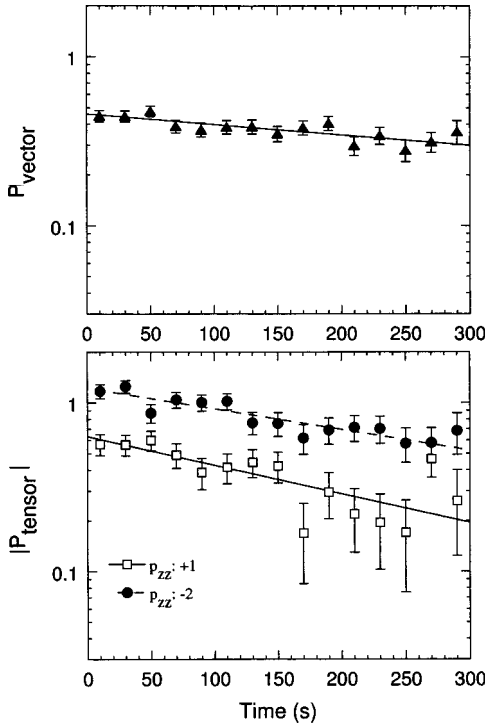


FIG. 4. Vector and tensor polarizations of the stored beam as a function of time. The solenoid frequency was 0.38 kHz away from the resonance. The lines are exponential fits.

unpolarized beam. While resetting the ring magnets and injecting beam for the next cycle, the solenoid is turned off. In order to improve statistics, data collected during ten Cooler cycles are added for each beam state.

It is obvious that by this method only polarization lifetimes that are comparable to the duration of a cycle (on the order of 100 s) are measurable. To achieve this, the distance  $\Delta f_{\text{sol}}$  to the resonance is chosen accordingly. The experiment was carried out at the three values for  $\Delta f_{\text{sol}} = 0.38, 0.20,$  and  $0.10$  kHz. The duration of the cycle was adjusted for best coverage of the decay of the polarization. The data are then binned in time such that the data-taking period is divided into about 15 bins. For the longest lifetime this results in bins 20 s wide while for the shorter lifetimes the bins are 4 s wide. The beam polarization for each spin state is then determined from the  $\phi$  distributions associated with each time bin as described earlier. As with the resonance search described above, the vector polarization results from beam states 1 and 2, the positive tensor polarization is an average over beam states 1–3, and the negative tensor polarization is obtained from beam state 4. Figure 4 shows  $P_z$  and  $P_{zz}$  as a function of time for  $\Delta f_{\text{sol}} = 0.38$  kHz away from the resonance.

In order to determine the lifetime  $\tau_p$  of the polarization an exponential function  $P(t) = P_i e^{t/\tau_p}$  was fitted to the vector and the two tensor polarizations as shown by the lines in Fig. 4. Figure 5 shows the vector and tensor polarization lifetimes as a function of the distance  $\Delta f_{\text{sol}}$  from the resonance. The lowest frequency ( $\Delta f_{\text{sol}} = 0.1$  kHz) is at approximately half the maximum of the resonance (see Fig. 3). As expected, the lifetimes for the two tensor polarizations are consistent with

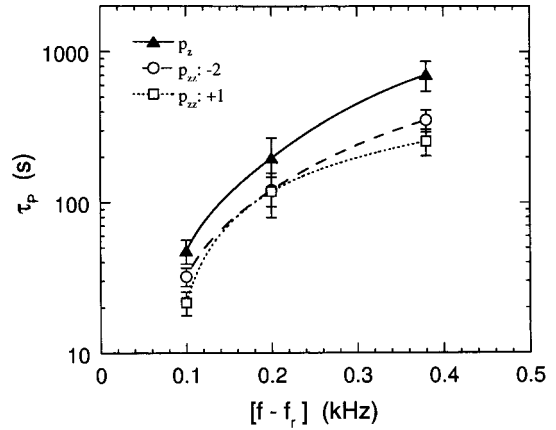


FIG. 5. Vector and tensor polarization lifetimes as a function of distance from the resonance. The curves are drawn to guide the eye.

each other. Since systematic errors decrease with increasing magnitude of the polarization, the agreement between the two measured tensor polarization lifetimes that differ in magnitude by a factor of 2 suggests that systematic errors are negligible. In the following we average the two values.

It is clear from Fig. 5 that vector polarization lasts longer than tensor polarization. Figure 6 shows the tensor polarization lifetime versus the vector polarization lifetime. The solid line represents the result of a least- $\chi^2$  fit of the points to a straight line going through zero. The ratio of the lifetimes resulting from this fit is  $\tau_{\text{vector}}/\tau_{\text{tensor}} = 1.9 \pm 0.2$ . The long-dashed line represents equal lifetimes while the short-dashed line represents a lifetime ratio of 3, which is the value one expects if transitions occur only between neighboring sub-states (Sec. VI and [6]).

### VI. THEORETICAL INTERPRETATION AND CONCLUSIONS

The beam polarization can be described in terms of the fractional populations ( $n_-$ ,  $n_0$ , and  $n_+$ ) of the three mag-

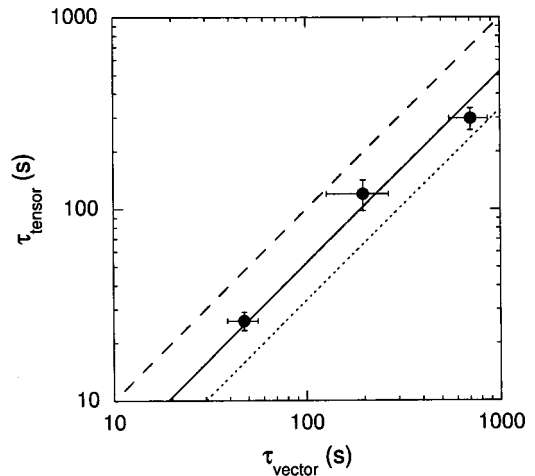


FIG. 6. Tensor versus vector polarization lifetime. The solid line is a least- $\chi^2$  fit through zero. The ratio of the lifetimes resulting from this fit is  $\tau_{\text{vector}}/\tau_{\text{tensor}} = 1.9 \pm 0.2$ . The long-dashed line represents equal lifetimes while the short-dashed line represents the theoretical maximum lifetime ratio of 3.0.



netic substates of the deuteron along a quantization axis that is along the spin alignment axis which coincides with the spin closed orbit. With  $n_- + n_0 + n_+ = 1$ , we have  $P_z = n_+ - n_-$  and  $P_{zz} = 1 - 3n_0$ .

Let  $q_1$  be the transition rate between neighboring substates ( $n_+$  and  $n_0$  or  $n_-$  and  $n_0$ ) and  $q_2$  be the transition rate between  $n_+$  and  $n_-$ . The evolution of the populations of the three substates is then described by

$$\begin{aligned}\dot{n}_+ &= -n_+(q_1 + q_2) + n_0q_1 + n_-q_2, \\ \dot{n}_0 &= -n_0(2q_1) + n_+q_1 + n_-q_1, \\ \dot{n}_- &= -n_-(q_1 + q_2) + n_0q_1 + n_+q_2.\end{aligned}\quad (6.1)$$

It is straightforward to calculate the derivatives of the vector and tensor polarizations:

$$\begin{aligned}\frac{dP_z}{dt} &= -(q_1 + 2q_2)P_z, \\ \frac{dP_{zz}}{dt} &= -3q_1P_{zz}.\end{aligned}\quad (6.2)$$

From this we get the ratio of the lifetimes

$$\frac{\tau_{\text{vector}}}{\tau_{\text{tensor}}} = \frac{3}{1 + 2q_2/q_1}.\quad (6.3)$$

This equation relates the ratio  $\tau_{\text{vector}}/\tau_{\text{tensor}}$  to the relative transition rates between substates. One can easily verify that if  $q_1$  and  $q_2$  were equal the vector and tensor lifetimes also would be the same. It is also clear that  $\tau_{\text{vector}}/\tau_{\text{tensor}} = 3$  is the theoretical maximum, attained when  $q_2 = 0$ . The ratio  $\tau_{\text{vector}}/\tau_{\text{tensor}} = 2$  that results from this experiment implies that  $q_1$  is four times larger than  $q_2$ . This result may help to understand the detailed depolarization mechanism, which at this time is unknown.

#### ACKNOWLEDGMENTS

We would like to thank J. M. Cameron, A. S. Belov, V. P. Derenchuk, G. W. East, D. L. Friesel, T. Rinckel, W. T. Sloan, and the entire Indiana University Cyclotron Facility staff for the successful operation of the Cooler Rinck with its new Cooler Injector Synchrotron and CIPIOS polarized ion source. We are grateful to B. B. Blinov, A. W. Chao, C. M. Chu, E. D. Courant, M. Q. Crawford, F. Z. Khiari, A. D. Krisch, S. Y. Lee, A. M. T. Lin, M. G. Minty, C. Ohmori, R. A. Phelps, R. E. Pollock, L. G. Ratner (deceased), T. Roser, H. Sato, T. Toyama, V. K. Wong, and others for their help with earlier parts of this experiment. This research was supported by grants from the U.S. Department of Energy and the U.S. National Science Foundation.

- 
- [1] W. K. Pitts *et al.*, in *Proceedings of the 9th International Symposium on High-Energy Spin Physics, Bonn, 1990*, edited by K. H. Althoff and W. Meyer (Springer, Berlin, 1991), p. 522.
- [2] H. O. Meyer *et al.*, *Phys. Rev. E* **56**, 3578 (1997).
- [3] B. von Przewoski *et al.*, *Rev. Sci. Instrum.* **69**, 3146 (1998).
- [4] H. Machner *et al.*, COSY Proposal No. 124, 2003 (unpublished); A. Kacharave *et al.*, COSY Proposal No. 126, 2003 (unpublished).
- [5] V. S. Morozov *et al.* (unpublished).
- [6] H. O. Meyer, *Nucl. Phys. A* **631**, 122c (1998).
- [7] V. P. Derenchuk and A. S. Belov, in *Polarized Gas Targets and Polarized Beams*, edited by R. J. Holt and M. A. Miller, AIP Conf. Proc. No. 421 (AIP, Woodbury, NY, 1998), p. 422.
- [8] W. Haeberli, *Annu. Rev. Nucl. Sci.* **17**, 373 (1967).
- [9] T. Rinckel *et al.*, *Nucl. Instrum. Methods Phys. Res. A* **439**, 117 (2000).
- [10] *The Madison Convention, Proceedings of the International Conference on Polarization Phenomena in Nuclear Reactions*, edited by H. H. Barshall and W. Haeberli (The University of Wisconsin Press, Madison, WI, 1971), p. XXV; see also S. E. Darden, *ibid.*, p. 39.
- [11] W. Haeberli, in *Nuclear Spectroscopy and Reactions, Part A*, edited by J. Cerny (Academic, New York, 1974), p. 151.
- [12] K. Sekiguchi *et al.*, *Phys. Rev. C* **65**, 034003 (2002).
- [13] V. A. Anferov *et al.*, *Phys. Rev. A* **46**, R7383 (1992).
- [14] H. O. Meyer *et al.*, *Nucl. Phys. A* **539**, 633 (1992).
- [15] B. Blinov *et al.*, *Phys. Rev. Lett.* **88**, 014801 (2002).